POLYMERS FOR ADVANCED TECHNOLOGIES
Polym. Adv. Technol. 2004; **15**: 144–148
Published online 2 February 2004 in Wiley InterScience (www.interscience.wiley.com). DOI: 10.1002/pat.422

PAT

Polyimides reinforced with the sol-gel derived organosilicon nanophase as low dielectric permittivity materials

Viktor Yu. Kramarenko[1], Tetyana A. Shantalil[2], Iryna L. Karpova[2], Kateryna S. Dragan[2], Eleonora G. Privalko[2], Valery P. Privalko[2]*, Daniel Fragiadakis[3] and Polycarpos Pissis[3]

[1]State Polytechnic University, 61002 Kharkiv, Ukraine
[2]Institute of Macromolecular Chemistry, National Academy of Sciences of Ukraine, 02160 Kyiv, Ukraine
[3]National Technical University of Athens, Zografou Campus, GR 15780 Athens, Greece

Received 15 March 2003; Accepted 3 July 2003

Polyimide (PI) nanocomposites prepared by the *in situ* generation of crosslinked organosilicon nanophase (ON) through the sol-gel process were characterized by densities, thermally stimulated depolarization currents and dielectric relaxation spectroscopy.

Both a looser molecular packing of PI chain fragments adjacent to the ON and a loose inner structure of the spatial aggregates of ON were assumed to be responsible for a non-additive decrease of the experimental values of dielectric permittivity for the nanocomposites. The pattern of composition dependence of the apparent dielectric permittivity of the ON suggested a probability of a morphological change around the composition PAAS/MTS = 100/16 (presumably, a sort of percolation transition from small-size, individual clusters into large-size, infinite clusters). Thus, PI reinforced with the sol-gel derived nanophase may have a reasonably good potential as low dielectric permittivity materials.

KEYWORDS: polyimides; nanocomposites; sol-gel technology; organosilicon nanophase; dielectric properties

INTRODUCTION

Sol-gel technology has become an attractive route for synthesis of polymer nanocomposites (PNs) with improved mechanical performance due to a homogeneous distribution of stiff inorganic nanoparticles (mostly, silica and its derivatives) throughout a continuous polymer matrix.[1–3] Obviously, further improvement of mechanical properties was not the major issue for the PN prepared from high-modulus, rigid-chain polymers like polymides (PIs); however, PI reinforced with the sol-gel derived nanoparticles proved competitive to commercial PI packaging materials due to their better gas permeation properties, higher heat resistance and flame retardance, etc.[4–8] So far, the potential of PI-based PNs as low dielectric permittivity materials, another traditional area of PI use,[9,10] remained uncertain, mainly due to a higher intrinsic dielectric permittivity of bulk silica ($\varepsilon' = 3.8–4.0$ at room temperature[11,12]) compared to that for neat PI ($\varepsilon' = 2.6–3.2$).[9,10] Somewhat unexpectedly, the values of $\varepsilon' = 2.5–2.8$ were reported for several series of PI-based PNs at relatively high contents of the sol-gel derived, silica-like nanoparticles.[13–15] These results combined with the relevant morphological data were interpreted as evidence for striking differences between the inner structures of bulk silica and of the aggregates of sol-gel derived nanoparticles.

According to our previous studies of a series of PI-based PNs by a variety of experimental techniques,[16,17] the crosslinked organosilicon nanophase formed by the sol-gel procedure possessed a rather loose inner structure characterized by the mean-square electron density fluctuations and by the dynamic elasticity moduli comparable to those of the pristine, glassy PIs. Thus, it seemed interesting to gain a further insight into the structure–property relationships for these PNs through measurements of densities, thermally stimulated depolarization currents and dielectric properties.

EXPERIMENTAL

Materials

Synthesis of PI-based nanocomposites has been described in detail elsewhere;[16, 17] therefore, only essentials need to be outlined here. In the first step, polyamic acid of molar mass 5000 with ethoxysilane end-groups (PAAS) was prepared by dissolution of 0.01044 mol of 4,4′-diaminodiphenyl ether and 0.025 mol of 3-aminopropyl triethoxysilane in 17.4 g of *N*,*N*-dimethyl acetamide, step-wise addition of 0.01169 mol of pyromellitic dianhydride to the solution and stirring at room temperature (r.t.) for 2 hr. Next, the precursors of nanocomposites (NCP) were obtained by addition of the required amount *S* (= 8, 20, ..., 120%) of

*Correspondence to: V. P. Privalko, Institute of Macromolecular Chemistry, National Academy of Sciences of Ukraine, 02160 Kyiv, Ukraine.
E-mail: privalko@iptelecom.net.ua

methyl triethoxysilane (MTS) to the solution, and stirring at r.t. for 10 hr. The homogeneous solutions were then cast on glass slides and stored at r.t. for at least 1 hr under humid conditions to ensure water absorption and MTS hydrolysis. Finally, the PAAS was imidized to the corresponding polyimide (PI) by step-wise heating and subsequent storage of the thin films of NCP for 2 hr at each of the following temperatures: 60, 100, 120, 150, 200, 250°C, and by post-cure for 5 hr at 300–315°C. The anticipated structure of the final product can be schematized as:

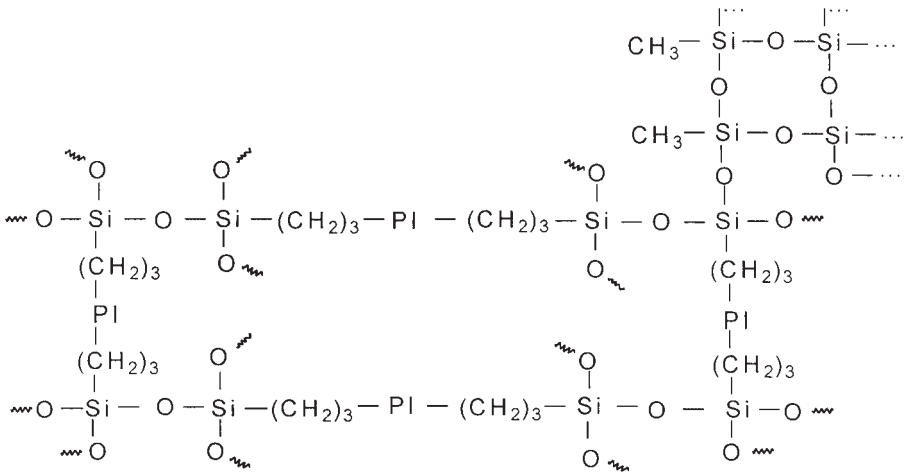

PI:

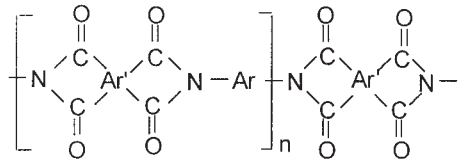

Ar'= 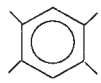 ; Ar= 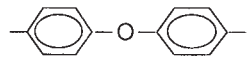

Taking due account of the quantities of water involved in the hydrolysis and condensation reactions, it can be readily shown that each 100 g of the precursor (PAAS) will yield 85.56 g of PI and 2.08 g of organosilicon nanophase (ON), while further addition of the MTS will result in the regular change of PI/ON mass ratios for different nanocomposites (Table 1).

Techniques

Thermally stimulated depolarization currents (TSDC) were measured in the temperature interval 100–300 K as described in detail elsewhere.[18–20] A disk-like specimen (diameter: 13 mm) placed between brass plates of a parallel capacitor was polarized by a d.c. electric field (field strength: 10 kV/cm) and cooled down (cooling rate: ~7 deg/min) to the liquid nitrogen temperature; then the field was switched off, the sample short-circuited and the TSDC were recorded (at the estimated equivalent frequency of 1.6×10^{-3} Hz) by an electrometer during heating to room temperature at a constant rate (~3 deg/min).

Complex dielectric permittivity, $\varepsilon^* = \varepsilon' - i\varepsilon''$, of disc-like specimens (diameter: 20 mm) sandwiched between gold-coated brass electrodes was measured over the frequency window 10^1–10^6 Hz in the temperature interval 173–293 K using several experimental setups,[18–20] including the

Table 1. Experimental and calculated densities of nanocomposites with different PAAS/MTS mass ratios

PAAS/MTS mass ratio	PI/ON mass ratio	Experimental density (g/cm^3)	PI/ON volume ratio[a] $(1-\varphi)/\varphi$	Calculated density[a] (g/cm^3)	Calculated ON density[b] (g/cm^3)
100/0	100/0	1.3882	100/0	1.3882	—
100/3	96.4/3.6	1.3866	97.4/2.6	1.4039	1.3259
100/8	94.4/5.6	1.3828	96.0/4.0	1.4127	1.2531
100/16	91.4/8.6	1.3825	93.8/6.2	1.4261	1.2962
100/40	83.3/16.7	1.3905	87.8/12.2	1.4631	1.4070
100/60	77.6/22.4	1.3668	83.3/16.7	1.4904	1.2601
100/100	68.3/31.7	1.3574	75.6/24.4	1.5375	1.2620
100/120	64.4/35.6	1.3393	72.3/27.7	1.5579	1.2119

[a]Assuming $\rho_{ON} = 2$ g/cm^3, $\rho_{PI} = 1.3882$ g/cm^3.
[b]Assuming $\rho_{PI} = 1.3882$ g/cm^3.

Table 2. Parameters of the γ-relaxation

PAAS/MTS mass ratio	T_γ (K)	$\Delta\varepsilon_\gamma$	$\Delta\varepsilon_m = \Delta\varepsilon_\gamma/(1-\varphi)$	$10^{-3}\Delta E_\gamma k^{-1}$ (K)	log f_0 (Hz)
100/0	146	0.169	0.169	5.7	14.1
100/3	141	0.277	0.284	—	—
100/8	141	0.273	0.288	—	—
100/16	140	0.262	0.284	5.3	13.6
100/40	139	—	—	—	—
100/60	133	0.225	0.281	4.9	13.4
100/100	135	0.228	0.318	4.7	12.2
100/120	123	0.234	0.344	4.2	12.2

Schlumberger frequency response analyzer (FRA 1260) supplemented by a buffer amplifier of variable gain (Chelsea dielectric interface) and the Hewlett– Packard 4284A Precision LCR meter.

Room temperature densities ρ were measured by a hydrostatic weighing technique in doubly-distilled water.

RESULTS AND DISCUSSION

Densities

As can be seen from Table 1, the experimental densities of the PN remained approximately composition-invariant up to PAAS/MTS=100/40, and started to decrease at higher MTS volume contents (φ). Judged by the glaring discrepancies between these experimental data and the densities calculated by the simple additivity rule (penultimate column in Table 1), the assumption on the identical densities (2.0 g/cm^3) for both the ON and silica[12] is not valid. The expected values of ρ_{ON} which were derived assuming composition-invariant ρ_{PI} (last column in Table 1), also look much too low. These results imply composition-dependent values of either ρ_{ON}, or ρ_{PI}, or both; the experimental evidence relevant to this preliminary conclusion will be discussed later.

Thermally stimulated depolarization currents

A single maximum on the TSDC traces in the limited temperature interval of our measurements for all studied samples, presumably, refers to the sub-glass (γ-) relaxation by the mechanism of non-cooperative, localized motions of an imide cycle.[9,10] As can be seen from Table 2, the γ-peak temperatures T_γ in the PN tended to decrease, while the relaxation strengths $\Delta\varepsilon_\gamma$ (estimated from the peak areas) increased, the higher the MTS volume content . Moreover, γ-relaxations could be also detected as maxima on the dielectric loss ε'' *v.* temperature diagrams at different frequencies (not shown); the corresponding Arrhenius plots for studied samples (Fig. 1) proved to be reasonably linear (in constructing these plots, the TSDC data from Table 2 at the equivalent frequency of 1.6×10^{-3} Hz were also used). As can be seen from Table 2, both apparent activation energies for γ-relaxation ($\Delta E_\gamma/k$) and pre-exponential factors (f_0) tended to decrease with the MTS content.

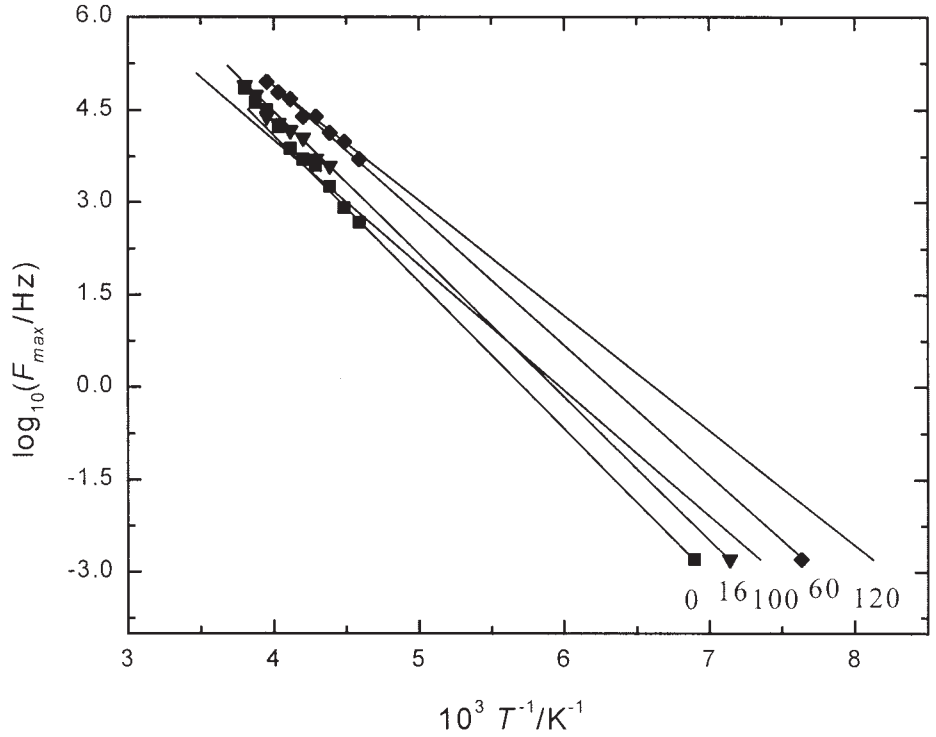

Figure 1. Arrhenius plots (numbers refer to the MTS contents, *S*).

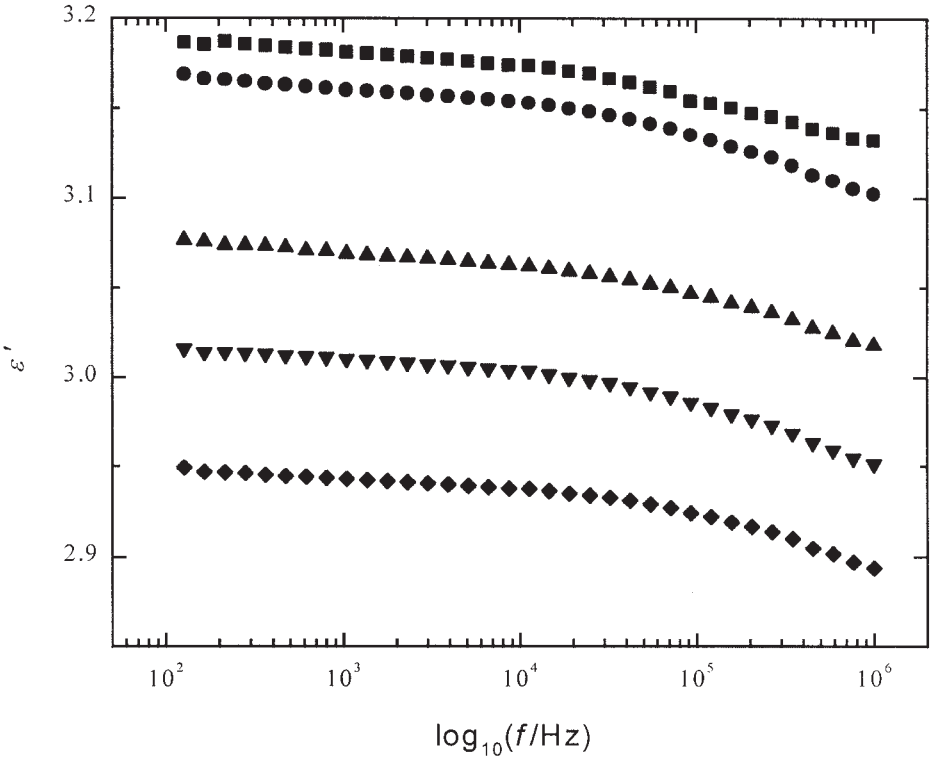

Figure 2. Frequency dependencies of the r.t. dielectric permittivities for the PNs with PAAS/m s ratios from 100/0 (uppermost curve) to 100/120 (lowermost curve).

The above data are clear evidence for the facilitated localized mobility of imide cycles in the PI matrix of PNs, which can be explained by looser molecular packing of PI chain fragments adjacent to the ON. Evidently, this effect (i.e. the apparent density deficit in the PI matrix) should become stronger, the higher the MTS content; however, the reliable estimate of its magnitude remains the issue of further studies.

Dielectric permittivity

As could be expected for dielectric materials in the temperature and frequency domains well outside the eventual structural relaxations,[21] the r.t. dielectric permittivity ε' for all studied samples is nearly constant over a reasonably broad interval of the driving frequency f, whereas on the approach to the γ-relaxation at $f > 1$ kHz it tended to decrease (Fig. 2). Moreover, the values of ε' (at a fixed frequency of $f = 1$ kHz) for the PNs decreased, the higher the MTS content (Table 3). This latter result is consistent with other relevant data[13–15] and can be regarded as further evidence for invalidity of a common-sense expectation of the increase of dielectric permittivity from $\varepsilon' \approx 3.18$ for the precursor (PAAS) to $\varepsilon' = 3.8$–4.0 for the bulk silica.

More quantitative assessment of the above data will be attempted within the frame of several theoretical treatments of dielectric permittivity–composition relationships for composite materials,[22] such as Looyenga model,

$$\varepsilon'^{1/3} = \varepsilon_m'^{1/3}(1-\varphi) + \varepsilon_i'^{1/3}\varphi, \quad (1a)$$

Lichtenecker model,

$$\ln \varepsilon' = \ln \varepsilon_m' (1-\varphi) + \ln \varepsilon_i' \varphi, \quad (1b)$$

and Stoltze *et al.*'s model,

$$\varepsilon'^{\alpha} = \varepsilon_m'^{\alpha}(1-\varphi) + \varepsilon_i'^{\alpha}\varphi. \quad (1c)$$

Implicit in Eqns (1a), (1b) and (1c) is the assumption that the dielectric permittivities of a matrix and of spherical inclusions (ε_m' and ε_i', respectively) remain composition-invariant, so that the volume fraction of inclusions and the fitting parameter α are the only factors responsible for the composition dependence of the dielectric permittivity of a composite (ε'). Therefore, although our data suggest that both a looser molecular packing of PI chain fragments adjacent to the ON (see the preceding paragraph) and a loose inner structure of the spatial aggregates of ON[16,17] may be responsible for a non-additive decrease of the experimental values of dielectric permittivity for the PN (Table 3), the values of ε' will be treated by Eqns (1a), (1b) and (1c) to derive the apparent values of ε_i' for the ON (assuming $\varepsilon_m' = \text{const} \approx 3.18$ for the PI).

As can be seen from Table 3, the apparent values of ε_i' estimated by different theoretical models exhibited a similar dependence on PN composition, remaining throughout considerably smaller than the dielectric permittivity of the bulk silica. Pragmatically, this result can be rationalized assuming that the ON is made up of nanoparticles of silica

Table 3. Experimental and calculated dielectric permittivities of nanocomposites

PAAS/MTS mass ratio	ε' (at 1 kHz)	ε_i (derived from Eqn) (1a)	(1b)	(1c)	α
100/0	3.18	—	—	—	—
100/3	3.16	2.45	2.47	2.24	2.05
100/16	3.07	1.68	1.81	1.78	0.01
100/40	3.01	1.96	1.95	1.90	0.57
100/60	2.94	1.93	1.93	1.89	0.49
100/100	2.94	2.27	2.15	2.11	1.54
100/120	2.91	2.27	2.15	2.11	1.58

($\varepsilon'_m = 3.8–4.0$) fused together into loose spatial aggregates with a considerable fraction φ_e of empty inner pockets ($\varepsilon'_i \approx 1$). As an illustrative example, the apparent values of φ_e estimated by the Looyenga model Eqn (1a) increased from ~0.40 for PAAS/MTS = 100/3 to ~0.65 for PAAS/MTS=100/16 and then decreased approximately linearly to ~0.45 for PAAS/MTS = 100/120. There is little doubt that the absolute values of φ_e derived in this fashion may be in serious error; nevertheless, the pattern of their composition dependence suggests a probability of a morphological change in the ON around the composition PAAS/MTS=100/16 (presumably, a sort of percolation transition from small-size, individual clusters into large-size, infinite clusters). Work is in progress to check this suggestion by electron microscopy experiments.

CONCLUSIONS

(1) Both a looser molecular packing of PI chain fragments adjacent to the ON and a loose inner structure of the spatial aggregates of ON is believed to be responsible for a non-additive decrease of the experimental values of dielectric permittivity for the PNs.
(2) The pattern of composition dependence of the apparent dielectric permittivity of the ON suggests a probability of a morphological change around the composition PAAS/MTS=100/16 (presumably, a sort of percolation transition from small-size, individual clusters into large-size, infinite clusters).
(3) PI reinforced with the sol-gel derived nanoparticles may have a reasonably good potential as low dielectric permittivity materials.

Acknowledgements

This work was supported by a NATO Fellowship grant through the Greek Ministry of National Economy awarded to V. Yu. Kramarenko, and by ''Thales'', NTUA.

REFERENCES

1. Mark JE, Lee CY-C, Bianconi PA. *Hybrid Organic-Inorganic Composites*, vol. 585. American Chemical Society: Washington, DC, 1995.
2. Schmidt H. Sol-gel derived nanoparticles as inorganic phases in polymer-type matrices. *Macromol. Symp.* 2000; **159**: 43–55.
3. Kickelbick G. Concepts for the incorporation of inorganic building blocks into organic polymer on a nanoscale. *Prog. Polym. Sci.* 2003; **28**: 83–114.
4. Joly C, Goizet S, Schrotter JC, Sanchez J, Escoubes M. Sol-gel polyimide-silica composite membrane: gas transport properties. *J. Membr. Sci.* 1997; **130**: 63–74.
5. Cornelius CJ, Marand E. Hybrid silica-polyimide composite membranes: gas transport properties. *J. Membr. Sci.* 2002; **202**: 97–118.
6. Chen Y, Iroh JO. Synthesis and characterization of polyimide/silica hybrid composites. *Chem. Mater.* 1999; **11**: 1218–1222.
7. Ahmad Z, Mark JE. Polyimide-ceramic hybrid composites by the sol-gel route. *Chem. Mater.* 2001; **13**: 3320–3330.
8. Liu J, Gao Y, Wang F, Wu M. Preparation and characterization of nonflammable polyimide materials. *J. Appl. Polym. Sci.* 2000; **75**: 384–389.
9. Bessonov MI, Koton MM, Kudryavtsev VV, Laius LA. *Polyimides—Thermally Stable Polymers.* Plenum Press: New York, 1987.
10. Wilson D, Stenzenberger HD, Hergenrother PM. *Polyimides.* Blackie: Glasgow and London, 1990.
11. Senkevich JJ, Desu SB. Poly(chloro-*p*-xylylene)/SiO_2 multilayer thin films deposited near-room temperature by thermal CVD. *Thin Solid Films* 1998; **322**: 148–156.
12. Todd MG, Shi FG. Validation of a novel dielectric constant simulation model and the determination of its physical parameters. *Microelectronics J.* 2002; **33**: 627–638.
13. Hedrick JL, Cha H-J, Miller RD, Yoon DY, Brown HR, Srinivasan S, Pietro RD, Cook RF, Hummel JP, Klaus DP, Liniger EG, Simonyi EE. Polymeric organic-inorganic hybrid nanocomposites: preparation of polyimide-modified poly(silsesquioxane) using functionalized poly(amic acid alkyl ester) precursor. *Macromolecules* 1997; **30**: 8512–8515.
14. Tsai M-H, Whang W-T. Low dielectric polyimide/poly(silsesquioxane)-like nanocomposite material. *Polymer* 2001; **42**: 4197–4207.
15. Liu W-Ch, *et al.* The structural transformation and properties of spin-on poly(silsesquioxane) films by thermal curing. *J. Non-Cryst. Solids* 2002; **311**: 233–246.
16. Shantalii TA, Karpova IL, Dragan KS, Privalko EG, Privalko VP. Synthesis and thermomechanical characterization of polyimides reinforced with the sol-gel derived nanoparticles. *Sci. & Technol. Adv. Mater.* 2003; **4**: 115–119.
17. Privalko VP, Shantalii TA, Karpova IL, Dragan KS, Privalko EG. Structure–property relationships for polyimides reinforced with the sol-gel derived organo-silicon nanoparticles. *Polym. & Polym. Compos.* 2003; **11**: 213–218.
18. Pissis P, Kanapitsas A, Savelyev YuV, Akhranovich ER, Privalko EG, Privalko VP. Influence of chain extenders and chain end-groups on properties of segmented polyurethanes. II. Dielectric study. *Polymer* 1998; **39**: 3431–3435.
19. Georgoussis G, Kyritsis A, Pissis P, Savelyev YuV, Akhranovich ER, Privalko EG, Privalko VP. Dielectric studies of molecular mobility and microphase separation in segmented polyurethanes. *Eur. Polym. J.* 1999; **35**: 2007–2017.
20. Georgoussis G, Kanapitsas A, Pissis P, Savelyev YuV, Veselov VYa, Privalko EG. Structure–property relationships in segmented polyurethanes with metal chelates in the main chain. *Eur. Polym. J.* 2000; **36**: 1113–1119.
21. Hedvig P. *Dielectric Spectroscopy of Polymers.* Adam Hilger: Bristol, 1977.
22. Stoltze S, Enders A, Nimtz G. Numerical simulation of random composite dielectrics. *J. Phys. I (France)* 1992; **2**: 401–410.